Research Article

Optimising Formability and Sustainability in AA6082 Stamping: A Numerical Approach Using AutoForm Simulations

Hakam Mohamed Fazeel[1], Li-Liang Wang[1]

[1]Department of Mechanical Engineering, Imperial College, London, United Kingdom

Abstract

High-strength aluminium alloys, particularly AA6082, are increasingly utilised in the automotive sector to achieve critical lightweighting targets. However, stamping these alloys presents significant formability challenges, including severe springback, excessive thinning, and wrinkling. This study investigates the numerical optimisation of AA6082 stamping processes using AutoForm Computer-Aided Engineering (CAE) simulations. By iteratively altering processing parameters—including forming temperature, blank shape, blank holder force, and forming speed—an optimised parameter set was established. Numerical section analysis demonstrated substantial improvements in part quality, yielding an 82.8% reduction in medium/high wrinkling, an 18.3% decrease in maximum springback, and a 6.5% improvement in minimum thickness. Furthermore, a comprehensive life-cycle and economic assessment revealed that the optimized parameters reduced manufacturing cycle times by 42.0%. This operational efficiency translated to a 30.9% decrease in per-part manufacturing costs and a 43.3% reduction in total CO_2 *emissions, proving that numerical optimisation can effectively harmonise mechanical performance with commercial and environmental sustainability.*

keywords AA6082, Sustainability, AutoForm, Formability Optimisation.

1. INTRODUCTION

Metals are some of the most used materials in everyday life and mass produced with millions of tonnes every year. With the global rapid transition towards sustainable manufacturing, many industries have promptly developed novel manufacturing technologies to reduce the global carbon dioxide emissions. Within the automotive industry, the most effective method of reducing carbon emissions is widely regarded as being through the use of lightweight materials. This involves reducing the weight of the Body-in-White using metals and manufacturing technologies for improved fuel efficiency within the transportation sector. A metal that is currently greatly emphasised in research are aluminium alloys.

Aluminium alloys stand out for their exceptional high strength-to-weight ratio and recyclability. Additionally, these alloys were available in abundance making them the ideal choice for use in the automotive industry. In 2024, China has produced a recorded 43 million tonnes of aluminium across a variety of sectors including automotive proving their large popularity in manufacturing. From the range of grades available, the 6000 series stands out for their mechanical strength of over 300 MPa, making alloys such as AA6082 commonly used for a car body (Liu and Wang 2025). Aluminium alloys such as AA6082 are manufactured using metal forming technologies, with the most used technique in the industry being stamping.

Stamping is the most common process when manufacturing a car, naturally leading to a large emphasis in recent literature and numerous advancements. Some of the most recent work demonstrating advancements with stamping include fast light alloy stamping technology (FAST) (Liu, Cai, et al. 2024) at Imperial College, capable of stamping parts at significantly reduced total energy cost and cycle times for each part. Rapid heating has led to increased properties in the formed part along with removing the need of an aging process entirely. Such advancements have demonstrated the capability

Author: Hakam Mohamed Fazeel <hakam.mohamed-fazeel25@imperial.ac.uk>

of optimising stamping processes to produce improved mechanical properties at a significant reduction in carbon dioxide emissions.

Various studies have been conducted in the recent years making major advancements in the technology that is used to reduce energy consumption and total cost of manufacture. However, very few studies have gone to quantify the reduction in costs as well as the reduction in carbon dioxide emissions through numerical simulation data based in China. Analysing stamping processes is crucial for identifying the areas causing the largest contributions for carbon dioxide emissions as well as costs during manufacturing. This study aims to set up a basic hot stamping process and then optimise certain parameters to define a process capable of improved or equivalent mechanical properties. A range of parameters may be considered including the blank shape, forming speed, heating temperature and blank holder force. The mechanical properties will be assessed by considering the distribution of mechanical thinning, springback, wrinkling, and formability limit diagrams provided by the AutoForm simulation. Finally, the collected data will be used to approximate the numerical cost and carbon emissions to produce a single part from both the base and optimised stamping process.

With the rapid growth of electric vehicles in the recent decades from China being imported to the rest of the world. This study will quantify the carbon dioxide emissions and costs based on the Zhejiang coastal province of China, known for cities such as Ningbo that play a large contributing factor in the automotive manufacturing industry.

2. NUMERICAL PROCEDURE

In order to evaluate the impact of various processing parameters on the resulting stamped part, a fully numerical approach was adopted using AutoForm hot stamping simulation. This approach reduces the time and money required, thus providing a more sustainable method of research and estimated results that can be later validated.

2.1. Setup of Base hot stamping process

2.1.1 Geometrical setup and Tooling Definition

Tooling geometries of a simple part as seen in Figure 1 were imported in the form of IGES and oriented via manual tipping. The tooling components were then defined with the following configuration:

- Die: Assigned the complete top-level tooling geometry
- Punch: Specified by isolating the inner central region of the tool cavity
- Binder: Defined by selecting the outer perimeter flanges

A constant force control was set to hold the binder consisting of a force of 5kN and additionally a cushion stroke was defined of 50mm.

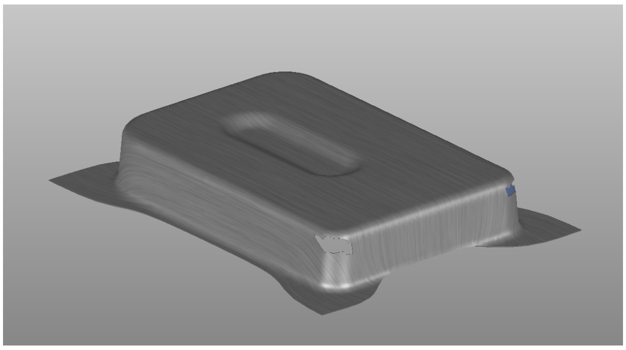

Figure 1. visual representation of the part used throughout the investigation

2.1.2 Material Characterisation and Blank Geometry

An experimentally validated thermo-mechanical material card from of the aluminium alloy AA6082 was obtained from the SmartForming platform and assigned to the blank. This material card is capable of producing reliable results regarding temperature dependent flow stress and strain-rate sensitivity of AA6082.

The blank has been defined to be a flat rectangular piece with dimensions of 375mm in length and 300mm in width. This piece was then modified to use rounded corners with a radius of 100mm to optimise the shape of the blank. Finally, the blank sheet was set to use a uniform thickness of 0.6mm.

2.1.3 Process Kinematics and Thermal Conditions

The virtual production line was constructed with three operational phases of Heating, Drawing and Cooling.

- Heating: The blank is initially heated to a temperature of 400 °C followed by a set transfer time of 1s
- Drawing: The mechanical press stroke was defined as 350mm over a forming time of 5s. The lubrication used during this process was defined as a Coulomb friction model under hot stamping conditions. The coefficient of friction was set using values provided by an interactive friction model from the SmartForming platform for reliable temperature dependent lubrication modelling.
- Quenching: Experimentally verified heat transfer coefficient (HTC) data was imported to the software. The in-die dwell parameters included a 1s delay following by a 1s long quenching action at a nominal quenching force of 100kN

2.1.4 Simulating and Data Extraction

Simulation was executed using AutoForm's CE+ solver with full field-data logging enabled. Key data including mechanical thinning, springback angles and localised wrinkling indices were extracted using drawn section plots across the part as shown on Figure 2. These will be exported in the form of CSV files and plotted against other forming parameters.

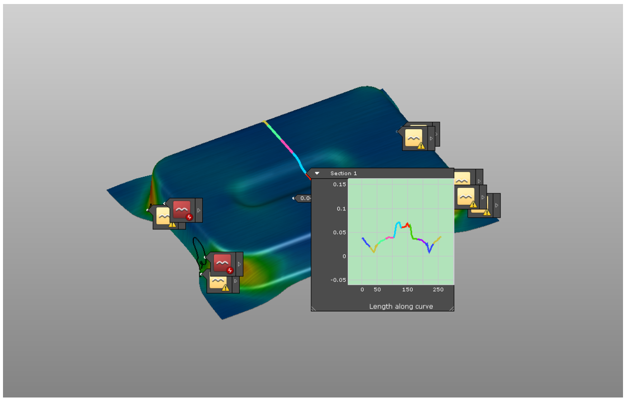

Figure 2. demonstration of data collection post simulation through AutoForm software

2.2. Parameter Optimisation

To achieve the optimal balance of formability and efficiency, various parameters of the CAE model were systematically changed. The primary manipulated variables included:

- Forming Temperature
- Blank Shape
- Blank Holder Force
- Forming Speed

The applied parameter change for the optimised processing profile will be discussed in the following text.

2.2.1 Temperature

According to literature, the currently set specified temperature of 400 °C will be above the recrystallisation temperature and therefore be considered as hot stamping. However, due to the high costs of energy and inefficiencies of heating, it is well recognised that temperatures contribute to a large portion of the costs and carbon emissions. Therefore, following numerous simulations it was decided to set the heated temperature of the blank to 250 °C. Additionally, as it takes over 20 minutes for AA6082 to recrystalise at 300 °C (Poletti et al. 2018), this optimised heating process would be considered as a warm stamping process (Liu and Wang 2025).

2.2.2 Blank Shape

The main concern regarding the blank shape stems from material waste as raw material is a significant contributor to the manufacturing cost. Overly large blank sizes will lead to an increased amount of material waste reducing the environmental sustainability and cost effectiveness of the process. Small optimisations in material blank shape may be able to significantly lower the cost per part and consequently significantly reduce the overall cost. Following this, numerous simulations were completed to identify an optimised blank size and finally deciding on dimensions of 340mm×275mm. This change results in a 16.9% from the original 375mm×300mm, likely contributing to a reduction in costs by a similar factor.

2.2.3 Blank Holder Force

The blank holder force is regarded as predominantly affecting the wrinkling and springback of the formed part. Following numerous simulations conducted in the past, it was decided to proceed by replacing the constant blank holder force with a controlled blank holder gap of 0.2mm.

2.2.4 Forming Speed

The forming speed, also described as the punch velocity would ideally be raised to reduce the cycle time of each part. A reduction in cycle times allows for a larger rate of production in an industrial setting. Additionally, literature has demonstrated through an experimental investigation that higher punch velocity benefits the quality of the formed part by reducing the springback angle (Krinninger et al. 2016). Following this, the punch velocity was set to increase from 75mm/s to 400mm/s. However, it is important to note that the literature also demonstrates that an increased punch velocity is capable of significantly reducing the quality if punch velocity is raised too far (Jung 1998).

2.3. Data Extraction and Evaluation

Numerical data regarding the material's structural response was extracted from the simulations using drawn section plots across the part. This data was subsequently analysed to identify the optimal processing parameters for maximizing part strength and surface quality.

2.4. Cost and Sustainability Analysis

The completed optimised profile for AA6082 stamping was compared against the base profile in comparative assessment considering the production cost and CO2 emissions for a single part. The following analysis follows a great simplification of the real world by only considering the largest factors contributing to the cost and CO2 emissions. Therefore, the cost and CO2 emissions were calculated for the raw material and the energy consumption for machinery separately and combined for an estimated total change (Gao et al. 2020). Energy rates for cost and emissions factor of CO2 were based from available data for a factory located in Ningbo, China.

2.4.1 Extracting base values

A set of base values from the AutoForm simulation results will be used to conduct the estimated calculations. These include base values used when setting up the base profile of stamping.

- Mass of material: vital value that is critical for finding estimates for the costs and CO2 emissions associated with the stamping process. A value for the mass of working material can be found through Eq. (1) taking into consideration the surface area, thickness of material and the density of AA6082. The surface area can be found by considering the length and width of the blank used in each profile, the thickness will be consistent between profiles and set as 0.6mm. Finally, the density of AA6082 will be found through online available data. The final values of mass for the base and the optimised profiles will be assigned as m_{base} and $m_{optimised}$ respectively.

$$m = A \times t \times \rho \tag{1}$$

- Thermal raise: Temperature change is another large contributor to the cost and CO2 emissions and will be taken into account. The respective temperatures for both the base and optimised profiles can be extracted directly from the AutoForm simulations and assigned to T_{base} and $T_{optimised}$ respectively.

2.4.2 Cost Analysis

The total cost of each part is defined as the sum of the cost of material and the cost of energy required for manufacturing. These cover the major costs but do not consider labour, maintenance and overhead which may raise the costs by a substantial amount. However, these will likely be the very similar for both the base and optimised profile and hence not taken into account for this investigation. The cost of material and required energy have been calculated in the following ways:

- Material Cost: The total cost of raw material ($C_{material}$) is directly related to the mass of blank (m) required for the operation. The unit cost of a blank will be found using the typical stock unit price of AA6082 assigned as $c_{material}$.

$$C_{material} = m \times c_{material} \quad (2)$$

- Energy cost: To find the cost of energy in GBP to heat the blank to the required temperature, the energy used for heating needs to first be found in Joules (Q). The required final heating temperatures is known for both profiles and will be used to calculate the energy required for heating by considering the specific heat capacity (c_p) of AA6082 in (3). This required energy in Joules can then be converted to power units and priced using the industrial electricity tariff (c_{energy}) in Ningbo, China using (4).

$$Q = m \times c_p \times \Delta T \quad (3)$$

$$C_{energy} = Q \times c_{energy} \quad (4)$$

2.4.3 Sustainability Analysis

The sustainability impact was quantified by calculating a minimum CO2 emission in kg for each part manufactured. The CO2 emission per part is simplified to be the sum of the CO2 emitted when manufacturing the blank material and the CO2 emitted to generate the power required for the heating process of the manufacturing.

- Material Emissions: Calculated by considering the carbon Emission Factor ($EF_{material}$) of bulk manufacturing 1kg of aluminium sheet. This was scaled by the recorded mass of the material with (5).

$$E_{material} = m \times EF_{material} \quad (5)$$

- Energy Emission: Similarly calculated using the carbon Emission Factor (EF_{energy}) of producing 1kWh of energy in China. This factor was used along with the required energy in kWh's to find emissions with (6).

$$E_{energy} = Q_{kWh} \times EF_{energy} \quad (6)$$

3. RESULTS

3.1. Mechanical Formability

3.1.1 Mechanical Thinning

Mechanical thinning and thickening behavior was evaluated across the critical drawn cross-section of the formed component. As shown in Figure 3, both forming profiles exhibited similar overall thickness trends, but the optimized parameters achieved a more uniform material distribution.

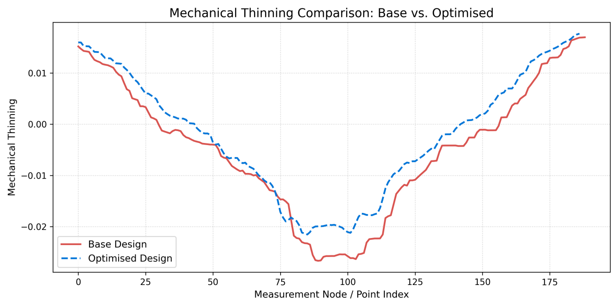

Figure 3. Variance of thickness across part, comparing the base stamping process (solid red) to the optimised process (dashed blue).

The maximum thinning percentage remained nearly identical between the two configurations, increasing marginally from 0.190 in the base profile to 0.194 in the optimized profile. However, the minimum thickness (representing maximum localized thickening/compression) improved from -0.217 in the base profile to -0.202 in the optimized design, representing a 6.5% improvement in localized thickness retention. This tighter variance demonstrates that reducing the forming temperature to 250 °C and implementing gap-controlled blank holding promotes more balanced material draw without inducing excessive localized necking or severe thinning. This information has been summarised into Table 1.

Table 1. Maximum and minimum mechanical thinning across the cross-section of the formed part from the base and optimised profiles.

	Base	Optimised
Maximum	0.19	0.194
Minimum	-0.217	-0.202

3.1.2 Springback

Springback angle variation across the part section profile is illustrated in Figure 4 and summarised in Table 2. Under the base hot stamping conditions (400 °C, 5 kN BHF), the part experienced significant elastic recovery post-unloading, reaching a maximum springback angle of 3.878°.

Table 2. Maximum springback angle in degrees for both base and optimised profiles.

	Base	Optimised
Maximum	3.878	3.170

By replacing the constant binder force with a controlled 0.2 mm blank holder gap and elevating the punch speed to 400 mm/s, the maximum springback angle was reduced to 3.170°. This represents an 18.3% overall reduction in maximum springback. The higher punch velocity minimizes the duration of thermal dissipation during active forming, while the gap control enforces consistent mechanical restriction, mitigating the stress gradients responsible for post-forming distortion.

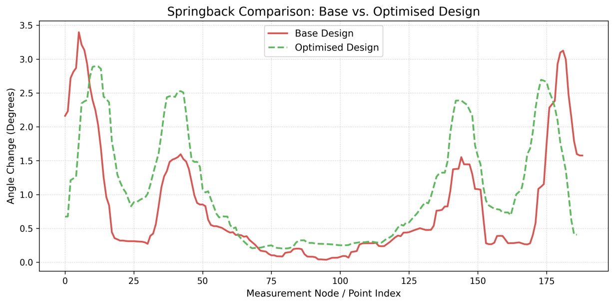

Figure 4. Variance of springback angle across part, comparing the base stamping process (solid red) to the optimised process (dashed blue).

3.1.3 *Wrinkling*

Localized wrinkling severity across the component surface was quantified using AutoForm's surface curvature and height indices, as plotted in Figure 5.

The base process exhibited pronounced flange and corner wrinkling, with medium severity wrinkling accounting for 0.99% of the total part area. Under the optimized warm stamping setup, medium-severity wrinkling was reduced to 0.17%, marking an 82.8% reduction in significant surface defects. While low-severity wrinkling increased from 6.80% to 16.54% due to lower forming temperatures, this was confined to non-critical trim zones. Overall, 83.29% of the part surface remained completely

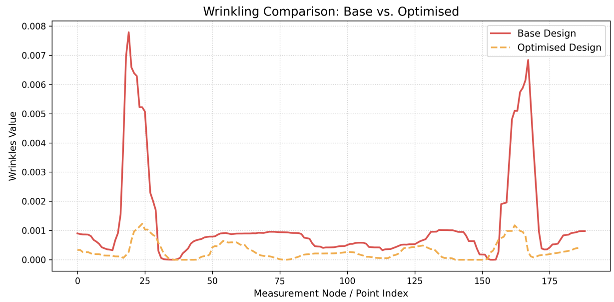

Figure 5. Variance of wrinkling across part, comparing the base stamping process (solid red) to the optimised process (dashed blue).

wrinkle-free while avoiding severe structural fluting, representing a major improvement in final part surface quality. The distribution of wrinkling categories has been filled in Table 3.

Table 3. Numerical distribution of the severity of wrinkling over the surface of the entire produced part.

	Base	Optimised
High	0	0
Medium	0.99	0.17
Low	6.8	16.54
No wrinkles	92.21	83.29

3.1.4 *Formability*

Material safety margins were evaluated for both the forming processes using the Formability Limit Diagram (FLD) generated by AutoForm. The FLD for the base and optimised profiles can be found in Figure 6 and Figure 7 respectively.

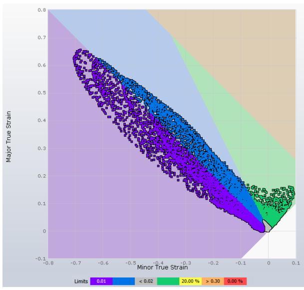

Figure 6. Formability Limit Diagram of base forming profile.

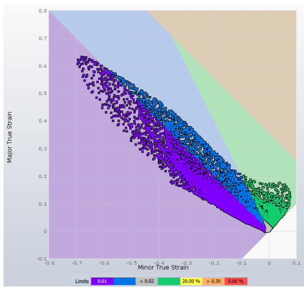

Figure 7. Formability Limit Diagram of the optimised profile.

Neither the base nor the optimized process resulted in any localized splitting or risk of splitting (0% for both cases), confirming that the blank deformation pathways remain safely below the Forming Limit Curve (FLC). The optimized process showed a slight redistribution in deformation modes: the area classified as "Safe" adjusted from 16.64% to 13.75%, while the ”Compress” region increased from 10.80% to 14.50%, and ”Insufficient Stretch” rose slightly from 36.29% to 38.53%. This shift confirms that the modified blank geometry (340 mm × 275 mm) and reduced warm-stamping temperature maintain high structural integrity while eliminating redundant material trim. The quantitative area distributions across formability zones are detailed in Table 4.

Table 4. Percentage value of the different categories of formability from AutoForm for both the base and optimised profiles.

	Base	Optimised
Thickening	36.27	33.21
Compress	10.8	14.5
Insufficient Stretch	36.29	38.53
Safe	16.64	13.75
Risk of Splits	0	0
Splits	0	0

3.2. Manufacturing Cost and Sustainability

The economic and environmental evaluations comparing the base hot stamping process to the optimized warm stamping process are summarized below. Firstly, the constants used in the cost analysis have been populated into Table 5.

Table 5. Constants used for cost analysis calculations.

	Value
Density / g/cm^3	2.7
Unit cost / £$/kg$	9.25
Specific heat capacity / $J/(kgK)$	896
Electricity tariff / £$/kWh$	0.072

The following constants could then be used to calculate various properties of the process and finalise with several approximations regarding the cost of manufacturing. These values have been populated into Table 6

Table 6. various data regarding the formed parts from the two forming profiles. (Anon, n.d.a, Anon, n.d.b).

	Base	Optimised
Temperature / $°C$	400	250
Mass / kg	0.18	0.15
Material cost / £	1.69	1.40
Energy required /kJ	61	31
Electricity Cost / £	1.23	0.61

By reducing the blank dimensions from 375 mm × 300 mm to 340 mm × 275 mm, raw material mass per blank decreased by 16.7% (from 0.18 kg to 0.15 kg), reducing per-part material cost from £1.69 to £1.40.

Furthermore, lowering the target heating temperature from 400 °C to 250 °C cut the thermal energy requirement (Q) nearly in half, from 61 kJ to 31 kJ per part. Based on regional industrial electricity tariffs in Ningbo, China, energy costs dropped from £1.23 to £0.61 per part. Combined, total direct manufacturing costs fell from £2.91 to £2.01 per part—a overall cost saving of 30.9%. This information has been summarised into Table 7 and visually represented on Figure 8

Table 7. The cost of manufacturing a single part broken down to the cost of aluminium and required energy for machinery. Costs included for both base and optimised setups

	Base	Optimised
Material	1.69	1.40
Energy	1.23	0.61
Total	2.91	2.01

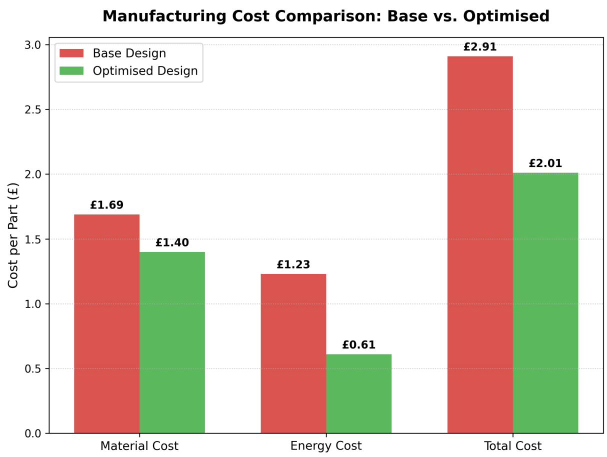

Figure 8. Visual comparison of costs of manufacturing a part in GBP between the base and optimised processing profiles

From a sustainability perspective, raw material carbon emissions (E_{material}) decreased from 2.69 kg CO_2 to 2.24 kg CO_2 per part due to material mass reduction. The primary environmental benefit, however, stemmed from energy savings (E_{energy}), which declined from 10.58 kg CO_2 to 5.29 kg CO_2 per part under the regional grid emission factor. In total, operational CO_2 emissions per stamped component dropped from 13.27 kg to 7.52 kg, achieving a total carbon footprint reduction of 43.3%. The emission factors used in the calculations can be found in Table 8.

Table 8. contains the emissions factors for both the material manufacturing as well as the emission factor associated with generating 1 kWh of energy. (Wu et al., 2025).

	Value
$EF_{material}$	0.62
EF_{energy}	14.77

The total carbon emissions have been summarised into Table 9 and visually plotted on Figure 9.

Table 9. Emitted CO2 in kg for manufacturing of aluminium and generation of power for factory use. CO2 emissions included for both base and optimised setups

	Base	Optimised
Material	2.69	2.24
Energy	10.58	5.29
Total	13.27	7.52

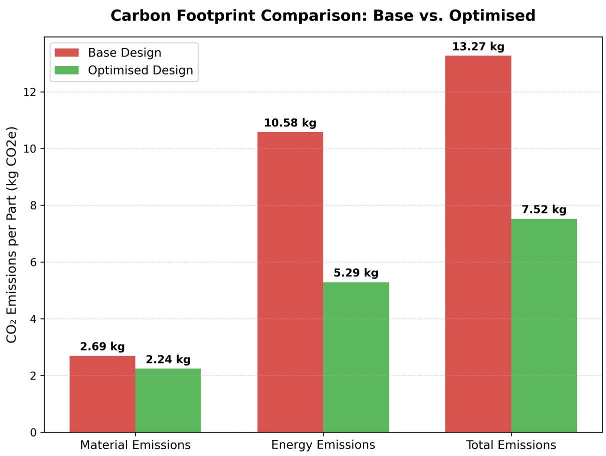

Figure 9. Visual comparison of CO2 emissions of manufacturing a single part between the base and optimised processing profiles

4. DISCUSSION

4.1. Assessing Change in Mechanical Properties

The study conducted demonstrates a significant number of ways in which cost and sustainability can be optimised at little cost of mechanical properties of the formed part. Key findings regarding the change in mechanical properties of the formed part have been populated into Table 10.

Table 10. Relative change in global values between the two manufacturing processes tested.

	% change
Max Thickness	2.1
Min Thickness	6.5
Max Springback	-18.3
Medium/High Wrinkling	-82.8

As seen from the results in Table 10. it is evident that the distribution of thickness in the formed part has stayed relatively consistent to the traditional process. Furthermore, the minimum thickness has increased by a large change than the maximum thickness demonstrating that the optimised process results in a small standard deviation of thickness distribution across the part.

The maximum springback has also experienced a reduction of 18.3% suggesting that the optimised part enables for a more accurate part to be formed. It is believed that this reduction in springback angle was seen as a result of increased quenching times and gap controlled blank holder force.

Finally, the level of significant wrinkling has also seen a major reduction of 82.8% suggesting that the optimised process provides higher surface quality parts.

4.2. Impact on Economics and Sustainability

The results displayed in Table 6 and Table 9 show that there is a clear link between the cost and the sustainability of a formed part. Therefore, optimising the sustainability of a formed part by reducing the material required and the energy required during production have a direct reduction in production cost. The largest reduction in both costs and carbon emissions stemmed from the large reduction in the heating temperature. Decreasing the temperature from 400°C to 250°C has caused the cost of heating and hence the carbon emissions to reduce almost proportionally. However, this study does not take into consideration the thermal and mechanical efficiencies of the processes involved during the manufacturing process.

4.3. Future Research

Future work is required to focus on a range of areas regarding this study. Some of the most notable of these areas is summarised in the text below.

- Most notable limitation stemmed from little experimental validation. Future work is required to manufacture the shown part using the parameters from this investigation and validate against numerically collected data.
- Consideration of the cost and time required to upgrade currently used industrial equipment. Industries likely haven't moved towards making the switch in their traditional stamping processes because of the downtime in their manufacturing, temporary losses and high costs included in upgrading the current stamping process. Further research is required to find the approximate period required to accumulate sufficient profits covering the large cost associated with upgrading current equipment.
- Insufficient data collected from the simulation of the formed part. Due to the time restrictions attached to this work, a limited amount of data was able to be collected from the formed part leading to a single section of data being collected. Additionally, each simulation required a significant amount of time to complete, adding a future restriction to the number of simulations conducted.

5. CONCLUSION

The research successfully developed a set of manufacturing parameters capable of producing an AA6082 aluminium part with similar properties to traditional hot stamping, but at heavily reduced costs, cycle times, and CO_2 emissions. Through careful control of forming temperature, blank holder force, speed, and blank geometry, severe forming defects were mitigated, including an 82.8% reduction in wrinkling and an 18.3% reduction in springback. Furthermore, this numerical optimization proves that structural integrity does not need to be sacrificed for process efficiency. The optimized process resulted in a 42.0% reduction in manufacturing cycle times, driving an estimated cost reduction of 30.9% and an environmental emissions reduction of 43%.

6. ACKNOWLEDGEMENTS

This research was generously funded by the Laidlaw Scholars Programme. The author would also like to thank Professor Li-Liang Wang, and the Metal Forming and Modelling Group at Imperial College for their continuous academic and technical support. This includes generous access provided to the SmartForming platforming containing validated material cards and interactive friction models.

References

Gao, M., Q. Wang, L. Li, and Z. Ma (Feb. 2020). "Energy-Economizing Optimization of Magnesium Alloy Hot Stamping Process". In: *Processes* 8.2, p. 186. ISSN: 2227-9717. DOI: 10.3390/pr8020186. URL: https://www.mdpi.com/2227-9717/8/2/186 (visited on 08/18/2026).

Jung, D. W. (Aug. 1, 1998). "Study of dynamic explicit analysis in sheet metal forming processes using faster punch velocity and mass scaling scheme". In: *Journal of Materials Engineering and Performance* 7.4, pp. 479–490. ISSN: 1544-1024. DOI: 10.1361/105994998770347620. URL: https://doi.org/10.1361/105994998770347620 (visited on 08/18/2026).

Krinninger, M., D. Opritescu, R. Golle, and W. Volk (Jan. 1, 2016). "Experimental Investigation of the Influence of Punch Velocity on the Springback Behavior and the Flat Length in Free Bending". In: *Procedia CIRP*. Research and Innovation in Manufacturing: Key Enabling Technologies for the Factories of the Future - Proceedings of the 48th CIRP Conference on Manufacturing Systems 41, pp. 1066–1071. ISSN: 2212-8271. DOI: 10.1016/j.procir.2015.12.137. URL: https://www.sciencedirect.com/science/article/pii/S2212827116000093 (visited on 08/18/2026).

Liu, H. and L.-L. Wang (Jan. 1, 2025). "2 - Review of advanced metal forming technologies". In: *Data Science in Metal Forming*. Elsevier, pp. 11–86. ISBN: 978-0-443-29145-6. DOI: 10.1016/B978-0-443-29145-6.00006-6. URL: https://www.sciencedirect.com/science/article/pii/B9780443291456000066 (visited on 08/17/2026).

Liu, X., Z. Cai, M. Ming, Q. Hou, X. Luan, H. Liu, L. Zhang, D. J. Politis, Q. Du, and L. Wang (June 30, 2024). "Fast light alloy stamping technology (FAST) for manufacturing lightweight pressings from dissimilar aluminium alloy-tailor welded blanks". In: *Journal of Manufacturing Processes* 120, pp. 1141–1156. ISSN:

1526-6125. DOI: 10 . 1016 / j . jmapro . 2024 . 05 . 021. URL: https : / / www . sciencedirect . com / science / article / pii / S1526612524004833 (visited on 08/17/2026).

Poletti, C., R. Bureau, P. Loidolt, P. Simon, S. Mitsche, and M. Spuller (Aug. 2018). "Microstructure Evolution in a 6082 Aluminium Alloy during Thermomechanical Treatment". In: *Materials* 11.8, p. 1319. ISSN: 1996-1944. DOI: 10.3390/ma11081319. URL: https://www.mdpi.com/1996-1944/11/8/1319 (visited on 08/17/2026).